Electronic Supplementary Material (ESI) for CrystEngComm.


# Supporting information

***S1. Alternative structure of RbAg4I5@SWNT with external octahedral positions occupied by silver atoms.***

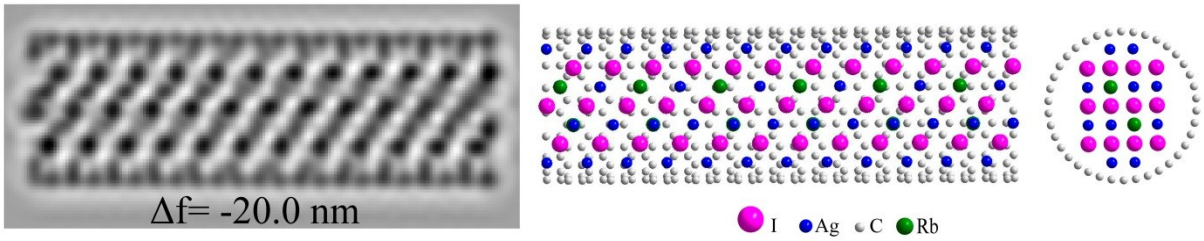


***S2. Additional experimental images and structure descriptions of $Rb_xAg_{1-x}I$@SWNT nanocomposites.***

| Composite | Experimental + models | Structure | Reference |
|---|---|---|---|
| RbI@SWNT | 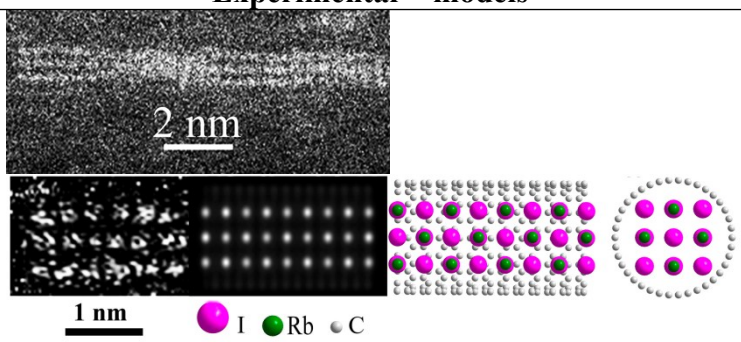 | *Pm3m,*<br>$d_1$ = 7.3 Å,<br>$D_{SWNT}$ = 1.4 Å | Present article |
| | (a)<br> 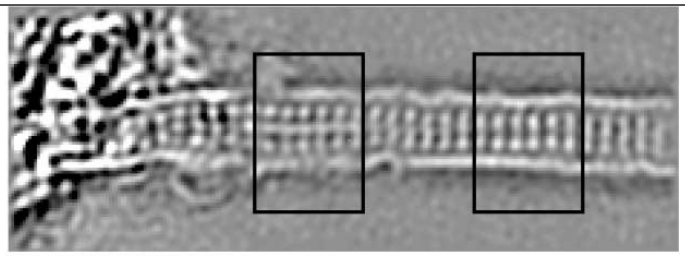 <br>(b)<br> 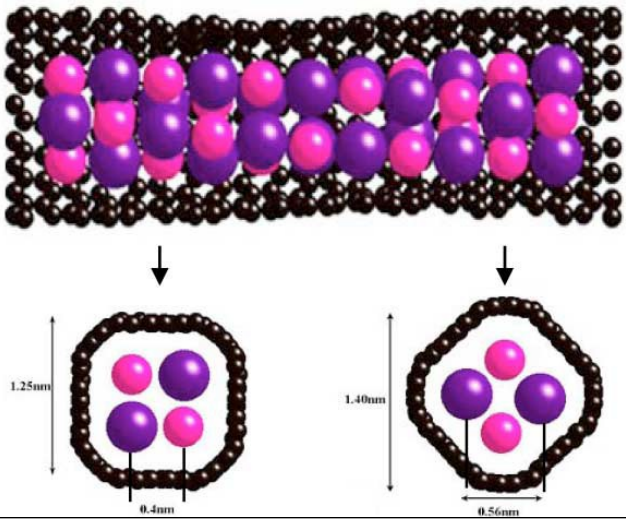 | Rocksalt<br>*a = b = c = 0.46 nm*<br>$D_{SWNT}$ = 1.35 Å<br>(17,0) | 1. A. Kirkland, et al. // 2005 Microsc. Microanal. 11, pp. 401–409. |

| | | | |
|---|---|---|---|
| AgI@SWNT | 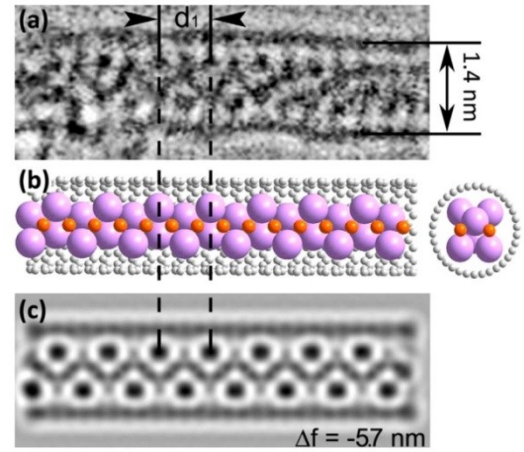 | $P\bar{2}mm$, $d_1$ = 7.5 Å, $D_{SWNT}$ = 1.32-1.4 nm | *1. A. Eliseev, et al.* // 2010, Carbon, V. 48 (10), pp. 2708-2721.<br><br>*2. A. Eliseev et al.* // Electronic Properties of Carbon Nanotubes, Ed. J.M. Marulanda, InTech, 2011, pp. 127-156. |
| | 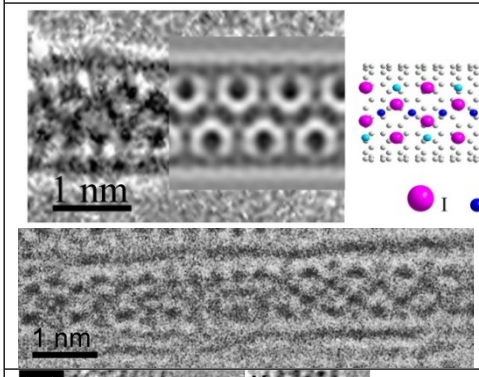 | $P\bar{2}mm$, $d_1$ = 7.5 Å, $D_{SWNT}$ = 1.4 nm | Present article |
| | 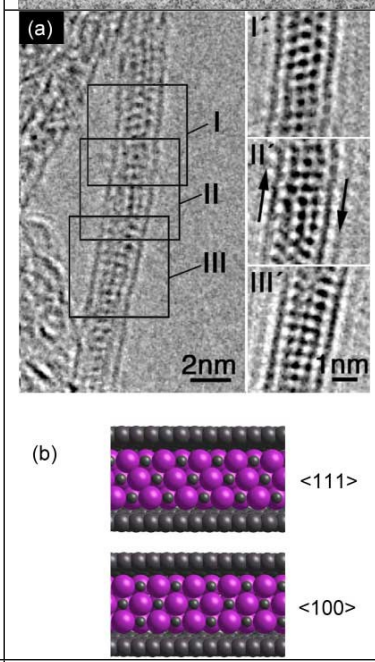 | Cubic $D_{SWNT}$ = 1.6 nm | 1. A. Kirkland, et al. // 2005 Microsc. Microanal. 11, pp. 401–409. |
| $RbAg_4I_5$@SWNT | 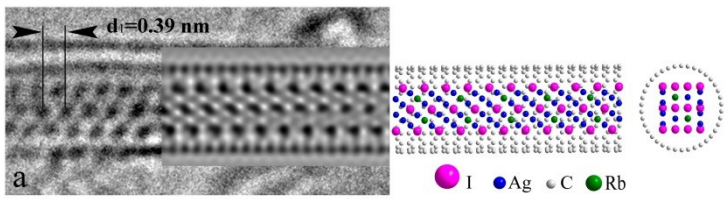 | Cubic (*fcc*) $d_1$ = 3.8 Å, $D_{SWNT}$ = 1.4 nm | Present article |

| | | | |
|---|---|---|---|
| | 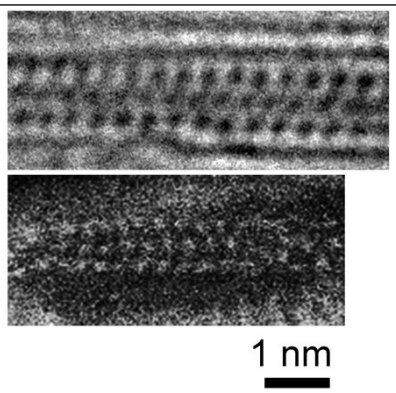 | | |
| | 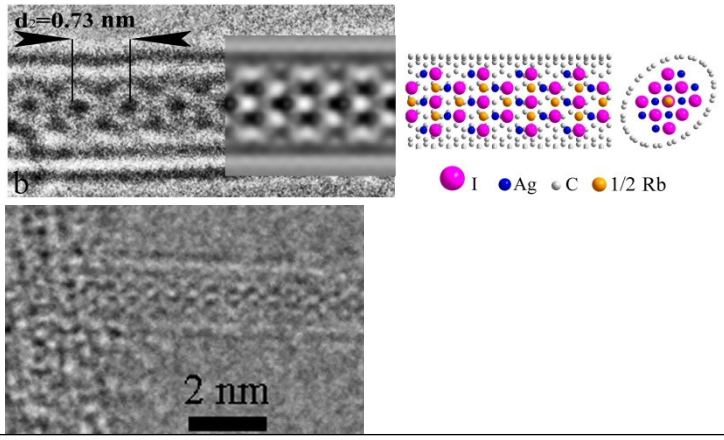 | Cubic (*fcc*)<br>$d_1$ = 7.3 Å,<br>$D_{SWNT}$ = 1.4 nm | |

***S3. Summary of Raman study.***

*Table S3. The positions of RBM- and G-lines in the Raman spectra of pristine SWNTs and nanocomposites at different laser excitation energies. The relative shifts of peak positions are given in the parentheses.*

| *Sample* | *Laser energy, eV* | *RBM-mode, $cm^{-1}$* | *G-mode, $cm^{-1}$* | *SWNTs diameter, nm* | *Conductivity type* | *Possible chiralities* |
|---|---|---|---|---|---|---|
| SWNT | 2.41 | 150.1 | 1553.8<br>1572.9<br>1592.9 | 1.52 | *m*-SWNT | (11, 11)*; (15, 6); (14, 8) |
| | | 164.8* | | 1.38 | *s*-SWNT | (11, 9)*; (15, 4)*; (12, 8) |
| | | 173.4 | | 1.31 | *s*-SWNT | (10, 9)*; (14, 4); (12, 7) |
| | 1.96 | 148.8 | 1542.3<br>1562.9<br>1590.9 | 1.53 | *m-SWNT* | (14, 8)*; (19, 1)*; (11, 11) |
| | | 164.6* | | 1.38 | *m-SWNT* | (10, 10)*; (13, 7)*; (14, 5) |
| | 1.58 | 153.5 | 1564.9<br>1587.7<br>1607.5 | 1.48 | m-SWNT | (15, 6)*, (16, 4), (12, 9) |
| | | 164.8* | | 1.38 | m-SWNT | (10, 10)*, (13, 7)*, (14, 5) |
| | | 184.5 | | 1.23 | s-SWNT | (15, 1)*; (10, 8); (11, 7) |
| RbI@SWNT | 2.41 | 169.6* (+4.8) | 1558.7<br>1571.1 (-1.8)<br>1594.1 (+1.2) | 1.34 | *s*-SWNT | (13, 6)*; (17, 0); (16, 2); |
| | | 181.6 (+8.2) | | 1.25 | *s*-SWNT | (10, 8)*; (11, 7); (15, 1) |
| | 1.96 | 154.0 (+5.2) | 1552.1<br>1567.5 (+4.6)<br>1590.7 (-0.2) | 1.48 | m-SWNT | (15, 6)*, (16, 4), (12, 9) |
| | | 168.6* (+4.0) | | 1.34 | m-SWNT | (14, 5)*; (15, 3); (16, 1) |
| | 1.58 | 165.9* (+1.1) | 1567.2 | 1.37 | m-SWNT | (10, 10)*; (14, 5); (13, 7) |

| | | | | | | |
|---|---|---|---|---|---|---|
| | | 179.7 (-4.8) | 1582.7 (-5.0)<br>1605.2 (-2.3) | 1.26 | s-SWNT | (16, 0)*; (13, 5); (14, 3) |
| $RbAg_4I_5$@SWNT | 2.41 | 170.4* (+5.6) | 1557.7<br>1572.1 (-0.8)<br>1597.2(+4.3) | 1.33 | *s*-SWNT | (13, 6)*; (12, 7); (17, 0) |
| | | 179.1 (+5.7) | | 1.26 | *s*-SWNT | (16, 0)*; (13, 5); (14, 3) |
| | 1.96 | 165.7* (+16.9) | 1552.1<br>1573.6 (+10.7)<br>1598.9 (+8.0) | 1.37 | m-SWNT | (10, 10)*; (14, 5); (13, 7) |
| | | 176.6 (+12.0) | | 1.28 | m-SWNT | (12, 6)*; (9, 9); (11, 8) |
| | 1.58 | 168.9 (+4.1) | 1568.4<br>1591.4 (+3.7)<br>1612.7 (+5.2) | 1.34 | m-SWNT | (14, 5)*; (15, 3); (10, 10) |
| | | 181.0* (-3.5) | | 1.25 | s-SWNT | (14, 3)*; (11, 7)*; (10, 8) |
| AgI@SWNT | 2.41 | 173.4* (+8.6) | 1558.3<br>1575.7 (-2.8)<br>1599.9 (+7.0) | 1.31 | *s*-SWNT | (10, 9)*; (14, 4); (12, 7) |
| | | 179.2 (-5.8) | | 1.26 | *s*-SWNT | (16, 0)*; (13, 5); (14, 3) |
| | 1.96 | 165.9* (+17.1) | 1554.6<br>1573.5 (+10.6)<br>1597.9 (+7.0) | 1.37 | m-SWNT | (10, 10)*; (14, 5); (13, 7) |
| | | 176.4 (+11.8) | | 1.28 | m-SWNT | (12, 6)*; (9, 9); (11, 8) |
| | 1.58 | 175.0* (+10.2) | 1583.3<br>1601.6 (+13.9)<br>1616.9 (+9.4) | 1.29 | m-SWNT | (12, 6)*; (9, 9); (11, 8) |
| | | 187.1 (+2.6) | | 1.21 | *s*-SWNT | (12, 5)*; (15, 1); (11, 6) |

**Predominantly excited type of SWNTs.*

***S4. Electrochemical Raman maps.***

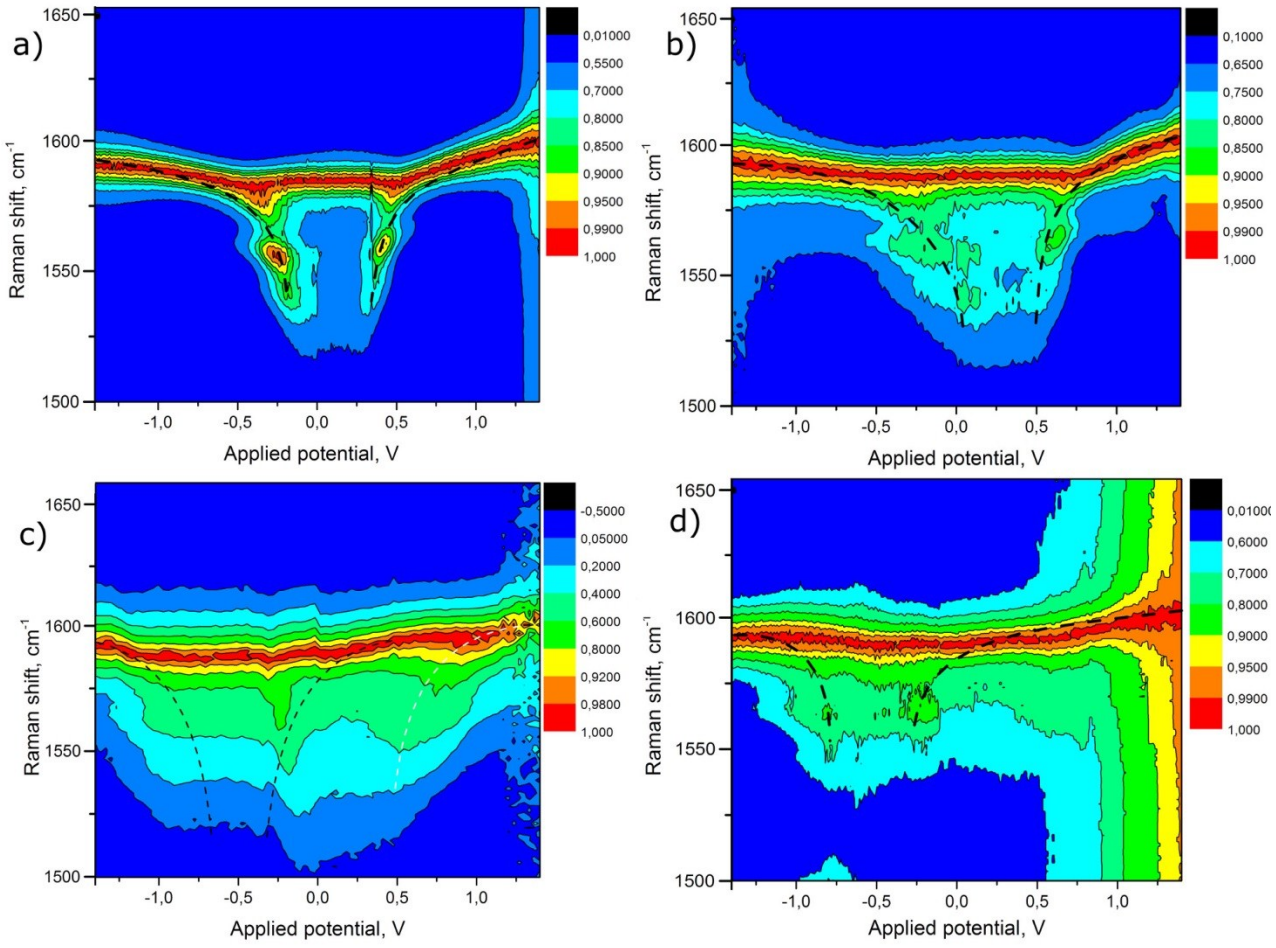

Spectroelectrochemical experiments were carried out in 0.2M solution of $LiClO_4$ in DME in potential rage of -1.4V – +1.4 V vs. Ag-pseudoreference electrode in potentiostatic staircase mode with a potential step of 5 mV. Black dashed lines represent Kohn anomaly of samples on the electrochemical Raman maps. a) Raw SWNT; b) RbI@SWNT; c) $RbAg_4I_5$@SWNT, white dashed line represents Kohn anomaly for raw SWNT; d) AgI@SWNT

***S5. Numerical results of XPS C 1s study.***

*Table S5. Summary of the results of the C 1s peak fitting.*

| *Sample* | *Feature* | *Relative intensity* | *Binding Energy, eV* |
|---|---|---|---|
| **SWNT** | *SWNT* | *0.887* | *284.50* |
| | *Ox* | *0.113* | *284.91* |
| **RbI@SWNT** | *SWNT* | *0.527* | *284.50* |
| | *Filled SWNT* | *0.383* | *284.71 (+0.21)* |
| | *Ox* | *0.089* | *285.10* |
| **$RbAg_4I_5$@SWNT** | *SWNT* | *0.218* | *284.50* |
| | *Filled SWNT* | *0.429* | *284.20 (-0.30)* |
| | *Ox* | *0.353* | *284.91* |
| **AgI@SWNT** | *SWNT* | *0.178* | *284.50* |
| | *Filled SWNT* | *0.584* | *284.22 (-0.28)* |
| | *Ox* | *0.238* | *284.91* |

***S6. The secondary electron cutoff spectra.***

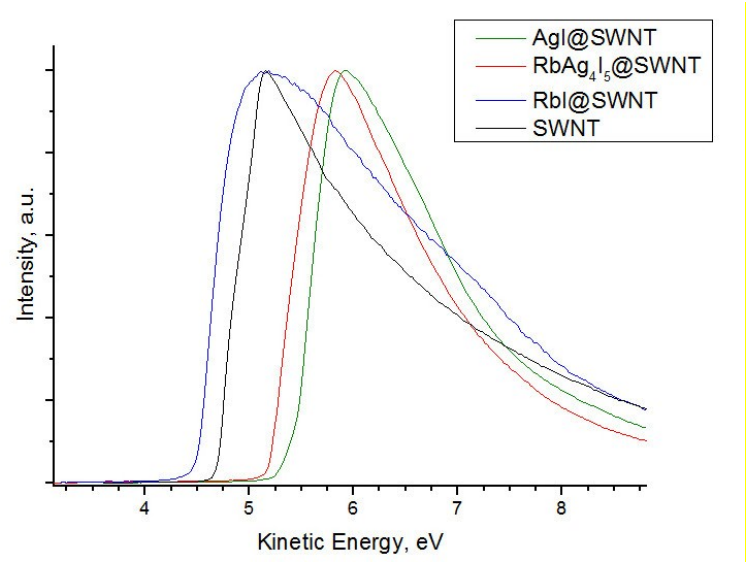


Secondary electron cutoff spectra recorded with the photon energy 75 eV. The graph shows noticeable deviation of electron work function of nanocomposites as compared to pristine SWNT. The values of electron work function were extracted as an intersection point of linear approximations of background and the secondary electron emission edge.